Catalina Eddies and Coastally Trapped Disturbances

WILLIAM C. SKAMAROCK, RICHARD ROTUNNO, AND JOSEPH B. KLEMP

National Center for Atmospheric Research, Boulder, Colorado*

(Manuscript received 19 October 2000, in final form 4 February 2002)

ABSTRACT

Observations show that coastally trapped disturbances (CTDs) often accompany Catalina eddies that appear in the southern California bight. In a previous modeling study of CTDs using simple environments and forcings, simulations of CTDs also evolved a mesoscale eddy that played a critical role in CTD formation and evolution. In this study the simple environments and forcings are extended to model the southern California bight, and simulations produce both Catalina eddies and CTDs. The simulated Catalina eddies and the mesoscale eddies in the previous CTD studies are dynamically equivalent. The primary mechanism for eddy formation in the simulations is lee troughing, and eddies and CTDs are produced provided that 1) there is sufficient stratification in the environment; 2) the offshore flow is of sufficient strength, breadth, and duration; and 3) there is sufficient terrain to produce significant lee troughing. The simulations show that CTDs can propagate out of the bight region when synoptic winds leading to eddy formation are northeasterly onto the bight, but are blocked by the prevailing marine layer northwesterlies for the case where the synoptic winds are northwesterly. Potential vorticity (PV) generated during the course of eddy formation does not significantly contribute to the eddy structure or CTD formation.

1. Introduction

Coastally trapped disturbances (CTDs) and Catalina eddies are two mesoscale flow phenomena occasionally observed along the United States west coast during the spring and summer months, and their appearance depends on synoptic-scale deviations from climatological flow and the presence of elevated terrain along the coast. In an earlier study, we showed that the essential dynamics of CTD formation and propagation can be captured in a simple model wherein an imposed offshore flow, mimicking the synoptic evolution, produces CTDs in an idealized coastal environment (Skamarock et al. 1999). In this paper, we present simulations demonstrating that Catalina eddies can be part of the phenomena described in our dynamical model for CTDs, and that Catalina eddies may lead to long-lived propagating CTDs depending on the orientation and position of the offshore flow relative to the coastal topography and the climatological northwesterlies in the marine layer.

CTDs are characterized by a southerly flow that interrupts the climatological northerly flow along the United States west coast. Low clouds, increasing pressure and lower temperatures often accompany CTDs. The southerly flow has a limited offshore scale and is rotationally trapped against the coastal mountains (Bond et al. 1996). Mass and Bond (1996) find that CTDs are produced when there is an eastward movement of the climatological central Pacific lower-tropospheric high into the Pacific Northwest, accompanied by westward movement of the climatological southwestern United States low. This synoptic evolution outlined by Mass and Bond implies geostrophic easterly offshore flow in Oregon and California. Using idealized simulations produced with a 3D nonhydrostatic model, we have shown that an imposed offshore flow will produce CTDs in idealized coastal environments (Skamarock et al. 1999). The imposed flow first weakens, through offshore advection, the prevailing northerly flow in the marine layer and lowers the pressure at the coast through lee troughing. The marine-layer flow around this low pressure evolves towards geostrophic balance, but is retarded as it encounters the coastal mountains to the south of the low and subsequently deepens the marine layer in this region. The elevated marine layer then begins progressing northward as a Kelvin wave and later may steepen into a bore or gravity current, this progression being the CTD. Many observed features accompanying CTDs are found in the numerical simulations, including the formation of a mesoscale pressure trough offshore and deep southerlies in the CTD at the coast. Also, stability in the atmosphere above the marine layer can give rise to topographically trapped Rossby waves that explain ob-

* The National Center for Atmospheric Research is sponsored by the National Science Foundation.

Corresponding author address: Dr. William C. Skamarock, NCAR, P.O. Box 3000, Boulder, CO 80307.
E-mail: skamaroc@ncar.ucar.edu

served propagating signals inland generally in phase with, but seemingly separate from, the CTD itself.

The climatology of the Catalina eddy events in the bight (Mass and Albright 1989) is similar in many aspects to the climatology of CTDs, except that the synoptic-scale offshore flow is from the northeast for CTD events, whereas the offshore flow is north-northwesterly onto the bight for the Catalina eddy events. Low pressure forms in both cases primarily because of lee troughing (Bosart 1983; Mass and Albright 1989) and the subsequent cyclonic circulations give rise to the Catalina eddy. CTD-like features in the bight can be found during many Catalina eddy events, for example in the 26–30 June 1988 case described in Mass and Albright (1989), and in the 4–7 June 1981 case outlined in Dorman (1985). Here we will show that the dynamics producing CTDs and Catalina eddies in our simulations are essentially the same, with the strength, direction, and location of the offshore flow relative to the bight determining whether or not a long-lived CTD is produced from an evolving Catalina eddy circulation.

We present an extension of the Skamarock et al. (1999) CTD model that accommodates the southern California bight region and climatological northwesterly marine-layer flow in section 2. In section 3 we show simulations that produce Catalina eddies for imposed northeasterly and northwesterly flow with dynamics similar to that described in past studies (i.e., lee troughing is the primary dynamical event in eddy formation). These simulations exhibit CTDs that propagate out of the bight for imposed northeasterly flow but not for imposed northwesterly flow. In section 4 we briefly examine the effects of different atmospheric initial states and imposed forcings on eddy and CTD formation. The Santa Ynez and San Rafeal mountains represent somewhat isolated terrain features to the north of the bight region. In section 4, we also briefly examine the effects of isolated terrain features within the context of the simplified simulations. In section 5 we consider eddy evolution from the potential vorticity perspective. A summary and discussion follow in section 6.

2. Idealization

In a climatological study of the summer season marine environment over the eastern Pacific, Neiburger et al. (1961) found that a stable marine layer almost always exists off the California coast during the summer season (see their Fig. 20). In their climatology, the mean inversion base intersects the coastal mountains at approximately 500 m above sea level and the inversion has a thickness of approximately 500 m. The marine layer deepens west of the coast with the inversion base rising to over 1500 m 1000 km offshore. The inversion thickness remains approximately constant but its strength weakens to the west (see Neiburger et al. 1961, Fig. 31). A geostrophically balanced along-coast flow accompanies this marine layer (not shown in Neiburger et al. 1961), with northerly winds achieving a maximum amplitude of approximately 10 m s^{-1} in the inversion at the coast.

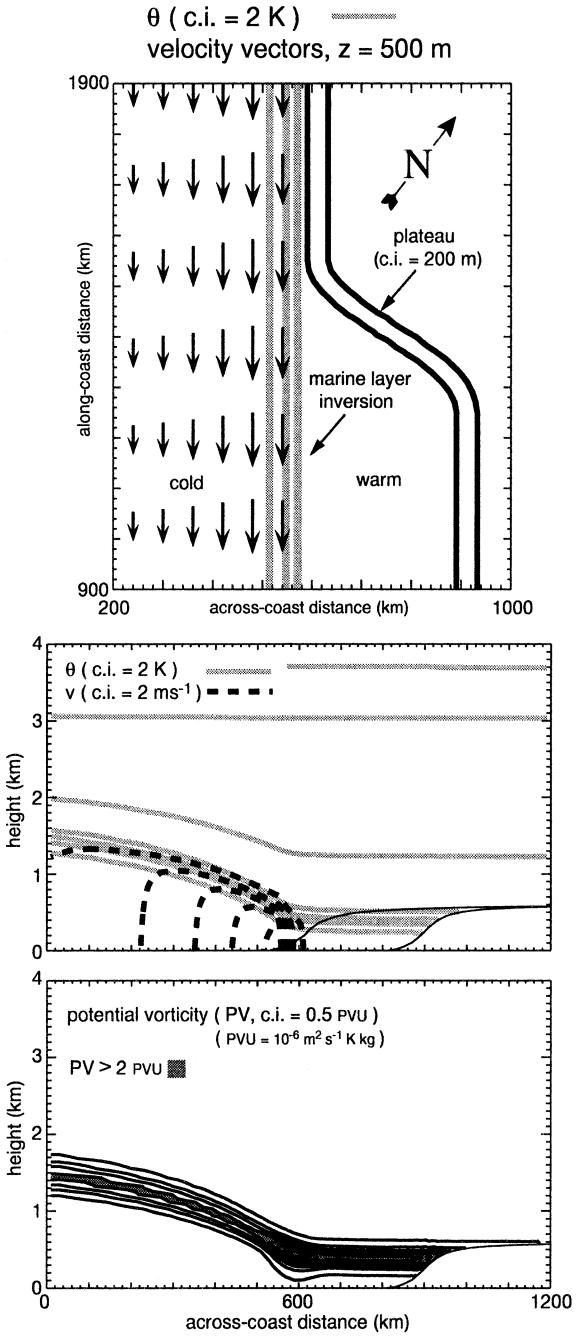

FIG. 1. Idealized climatological basic state. Depicted are horizontal (top) and vertical (middle) cross sections of horizontal velocity and potential temperature, and a vertical cross section (bottom) of the initial-state potential vorticity.

Our idealization of the climatological mean state is depicted in Fig. 1, and over it is superposed an idealized coastal mountain topology that includes the California bight. This state is the same as in Skamarock et al.

(1999) except for the addition of the bight topology. We have rotated the coordinate system clockwise around the vertical axis such that the coastline to the north of the bight is parallel to the y axis in Fig. 1, and extends off to the northwest as do the actual coastal mountains north of the bight. The inversion is modeled after the climatology of Neiburger et al. (1961), although we do not weaken the inversion to the west as in the climatology. Contrary to the climatology (Zemba and Friehe 1987; Dorman et al. 2000), our northwesterly flow is constant with height in the marine layer because we do not include the complicating effects of surface drag and surface heat fluxes, nor does it vary in the along-coast direction. The mean potential temperature profile is less stable below 2500 m, and reflects observations (Ralph et al. 1998) showing the atmosphere to be more weakly stratified in a 1- to 2-km-thick layer above the marine inversion preceding and during many of the CTD events. Also, the marine layer does not decrease in height progressing into the bight and to the south as observed (Dorman and Winant 2000).

The terrain to the north and east of the bight also represents an idealization of the actual terrain. We model the coastal terrain and the mountains surrounding the bight as a constant height plateau, whereas in the actual topography there are significant variations in the slope and maximum height of the coastal mountains and in the mountains surrounding the bight.

3. Simulations in the idealized California bight environment

We have performed simulations integrating the nonhydrostatic compressible equations using a model similar to that described in Durran and Klemp (1983), but with the addition of a semi-Lagrangian monotonic integration scheme for the potential temperature θ. The semi-Lagrangian scheme uses the tensor product of 1D Hermite polynomials with the cubic derivative estimate for interpolations as described in Williamson and Rasch (1989), and the interpolators are rendered monotonic using their condition (2.19). The monotonic scheme for θ is needed in order to maintain the sharp marine inversion; the centered-in-space-and-time leapfrog scheme requires excessive numerical filtering (that would remove the marine layer and inversion over time) to remove noise generated at the inversion and CTD edges. Using the monotonic semi-Lagrangian scheme, we have removed all explicit numerical filters and dissipation in the θ equation, and we use only a horizontal fourth-order filter in the momentum equations.

We impose either an northeasterly or northwesterly offshore flow onto the idealized California bight over a finite-length region in the 3D simulations to mimic the offshore flow in the synoptic evolution in Catalina eddy events. The flow has the form

$$U_{\text{imposed}} = U_o \sin^2\left(\pi \frac{t}{T}\right) \times \cos^2\left(\pi \frac{y - y_c}{L_e}\right), \quad (1)$$

where the parameters are $U_o = 4$ m s^{-1}, $T = 3$ days, the width of the imposed flow $L_e = 600$ km, $U = 0$ for $|y - y_c|/L_e > 1/2$, and $y - y_c$ is the distance from the centerline. The imposed offshore wind is uniform in the offshore direction and in z, and is assumed to be balanced by a pressure gradient that is also imposed in the model, hence the imposition of this flow does not engender any geostrophic adjustment in and of itself. We do not include a temperature gradient with this balanced flow because to first-order (Boussinesq) no temperature gradient is indicated as there is no vertical shear. The simulation domain has a southeast–northwest length of 2400 km, an across-coast length of 1200 km, and the finite-difference grid has $\Delta x = \Delta y = 20$ km. Open boundary conditions are imposed at all lateral boundaries and a radiation condition is used at the upper boundary located at $z = 4$ km. The lower boundary is free-slip over both the land and ocean surfaces.

Our idealized initial state is a steady-state solution to the equations of motion and that is a close representation of the observed climatological flow. The imposed perturbations described by (1) are idealizations of the large-scale flow perturbations observed in the climatology of CTDs and Catalina eddies documented by Mass and Albright (1989). As we will show, these perturbations lead to the formation of Catalina eddies and CTDs in our simulations. Beginning with a steady initial state, the fact that the perturbations lead to the phenomena (eddies and CTDs) that possess the proper time and length scales provides strong evidence for a cause and effect relationship between the perturbations (in this case the imposed offshore flows) and the eddies and CTDs.

a. Catalina eddy simulation

Figure 2 shows horizontal cross sections of the horizontal wind vectors, potential temperature, and pressure at 250 m above the sea surface for days 1 through 3, where the imposed flow is northwesterly onto the bight. At 1 day there is a noticeable depression in the marine layer centered slightly west of the offshore flow maximum, with a slight acceleration of the northwesterly flow to the west of this depression. In response to this low pressure, the flow turns northeast into the bight and impinges on the coastal topography to the east-southeast. The development of the marine layer depression and associated low pressure is qualitatively the same as that occurring in our idealized CTD simulations (see Skamarock et al. 1999, Fig. 3), and is a manifestation of lee troughing associated with the imposed offshore flow and coastal topography. This lee-troughing mechanism is consistent with the lee-troughing mechanism observationally inferred by Bosart (1983), Mass and Albright (1989), and others investigators.

Over the next day the depression in the bight has grown

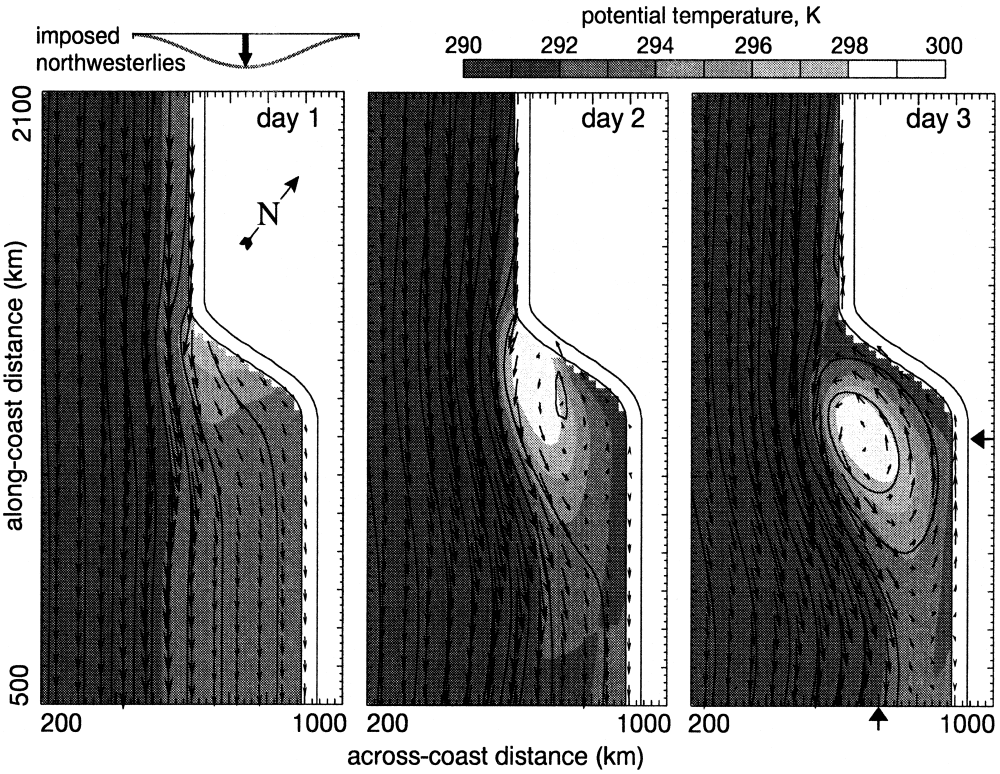

FIG. 2. Horizontal cross sections at $z = 250$ m for the simulation using an imposed northwesterly flow (the Catalina eddy simulation). Potential temperature θ is contoured in gray (contour interval = 2 K) and pressure is contoured using solid lines with a contour interval of 0.5 mb. Maximum vectors are approximately 14 m s^{-1} in the plots. The bold arrows at day 3 denote locations of the vertical cross sections shown in Fig. 3.

substantially (Fig. 2, day 2), and the pressure low has deepened. The potential temperature is dropping to the east of the depression along the coast in the area where the marine layer is deepening. A region of east-southeasterly winds is developing in response to the pressure gradient found at the northern edge of this area where the coastal marine layer is deepening. This flow develops in a similar manner to that observed in the case of a straight coastline (see Skamarock et al. 1999, Figs. 4 through 6), and is the first manifestation of a CTD.

By day 3, the region of marine-layer deepening and its associated east-southeasterly flow (the CTD) have spread throughout the coastal region in the bight. At the northwestern edge of the bight, the CTD has encountered the climatological northwesterlies and its progression has been halted. The disturbance in the bight now takes the form of a Catalina eddy with elevated marine-layer heights along the coast in the bight, a marine-layer depression offshore in the bight, and a closed cyclonic circulation.

The vertical structure of the eddy at day 3 is shown in Fig. 3. The eddy does not extend above the top of the plateau; it is largely confined to the marine layer. The circulation center coincides with a depression in the marine layer and low pressure (not shown). The limited vertical extent of this simulated eddy and its horizontal scale of a few hundred kilometers is consistent with Catalina eddy observations (Bosart 1983; Wakimoto 1987; Mass and Albright 1989) and simulations of observed cases (Ueyoshi and Roads 1993; Thompson et al. 1997; Davis et al. 2000) and other more idealized simulation results (Ulrickson et al. 1995).

b. CTD simulation

Figure 4 shows horizontal cross sections of the horizontal wind vectors, potential temperature and pressure at 250 m above the sea surface for days 1 through 3, where the imposed flow is northeasterly onto the bight, as opposed to northwesterly (Fig. 2). In this case the marine-layer depression begins to form around the northwestern tip of the bight region as compared to the depression in the previous case that is located farther to the east. There is no significant flow into the bight. At day 2 there is weak southeasterly flow and some elevation of the marine layer in the southeastern coastal region of the bight; this is the incipient CTD. The climatological northwesterly marine layer flow, while accelerated somewhat, is being displaced away from the coast north of the bight. The cyclonic circulation farther to the southeast represents the incipient Catalina eddy.

By day 3 the southeasterlies and elevated marine layer

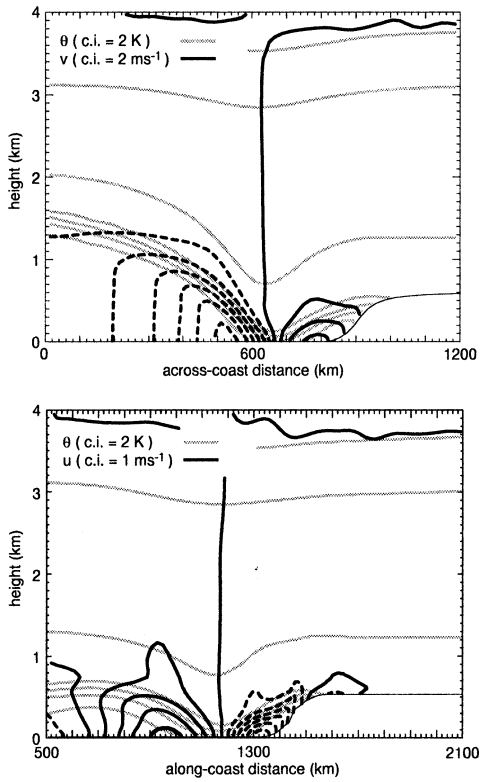

FIG. 3. Vertical cross sections depicting the eddy structure at day 3 in the simulation. The cross sections are located at $y = 1200$ km (top) and $x = 700$ km (bottom), and the locations are denoted by the bold arrows in Fig. 2.

in the bight region have propagated through the bight region and are now propagating up the coast as a CTD. A Catalina eddy is still evident in the bight, and its structure is vertically confined to the marine layer. It possesses a less pronounced depression offshore, a weaker circulation, and is located farther south and farther offshore relative to the eddy in Fig. 2 that was produced from northwesterly offshore flow.

4. Eddy and CTD formation

We have performed numerous tests using this model varying the structure of the imposed flow, the initial environment, and the terrain. We find that eddies and CTDs are produced in the bight as long as 1) there is sufficient stratification in the environment; 2) the offshore flow is of sufficient strength, breadth, and duration; and 3) there is sufficient terrain to produce the significant lee troughing.

The findings concerning the stratification and offshore flow are illustrated in results from three simulations presented in Fig. 5, where horizontal cross sections at day 3 and $z = 250$ m are plotted for each simulation. The first simulation (Fig. 5, left panel) uses an imposed northwesterly wind over the entire domain, removing only the length-scale dependence from the imposed flow given by (1), and uses an initial state that does not contain northwesterly flow in the marine layer (there is no flow in the initial state); the initial marine layer has a constant height of 400 m. As compared with our reference simulation given in Fig. 2, both an eddy and CTD are produced. In this case, however, the CTD propagates up the coast because there is no marine layer wind to obstruct it. The second simulation (Fig. 5, middle panel) is identical to the first, except that the imposed flow retains the spatial structure given by (1). A somewhat smaller eddy is produced compared with the first simulation, and both produce CTDs that propagate up the coast.

The third simulation uses the imposed flow from (1) along with a constant stability atmosphere with $N = 10^{-2}$ s^{-1}; there is no marine layer, no inversion and no flow in the initial state. Again an eddy forms, but it is somewhat weaker compared with simulations using a prescribed marine layer. This result is expected given the lee trough dynamics and the weaker stratification in the environment. We would also like to point out that the simulations results depicted in Fig. 5 demonstrate that neither horizontal vorticity present in the climatological marine layer flow, nor horizontal vorticity present in the imposed flow are necessary for production of an eddy or a CTD.

We have also performed many simulations varying the strength and duration of the imposed offshore flow. The results (not shown) are consistent with lee-trough theory (see Pierrehumbert 1986, 509–511). Lee troughing is a low Rossby number phenomena [$U/(fl) \leq 0.1$], thus for a length scale of a few hundred kilometers (the scale of the bight) and $f \sim 10^{-4}$ s^{-1}, the velocity U should be a few meters per second [for $U/(fL) \sim 0.1$]. The timescale of the imposed flow will be approximately L/U, that is a few days in this case. This scaling was used to construct the imposed flow given by (1). As shown earlier, the horizontal length scale of the imposed flow is not important as long as the flow is sufficiently broad, generally $L_e > L$ in (1). We have found that an eddy does not form if the timescale of the imposed flow in (1) is too short because there is not sufficient displacement of the marine layer. Additionally, lee-troughing perturbations get advected downstream and the model does not produce a recognizable eddy if the timescale is too long or the imposed velocity too strong. Flow separation can also occur (and no lee troughing) if the imposed velocity is too strong [i.e., $U/(fL)$ is too large; see Fig. 3 of Skamarock et al. 1999].

The terrain used in the first two simulations enables coastal trapping of the marine layer, and the vertical structure of the eddies and CTDs is limited to the marine layer and does not extend above the plateau height of 600 m. The San Rafael, San Gabriel, and San Bernardino mountains are isolated mountain ranges located north of the bight region that extend significantly higher than 600 m, and they could have a significant influence on the northwesterly or northeasterly flow we impose

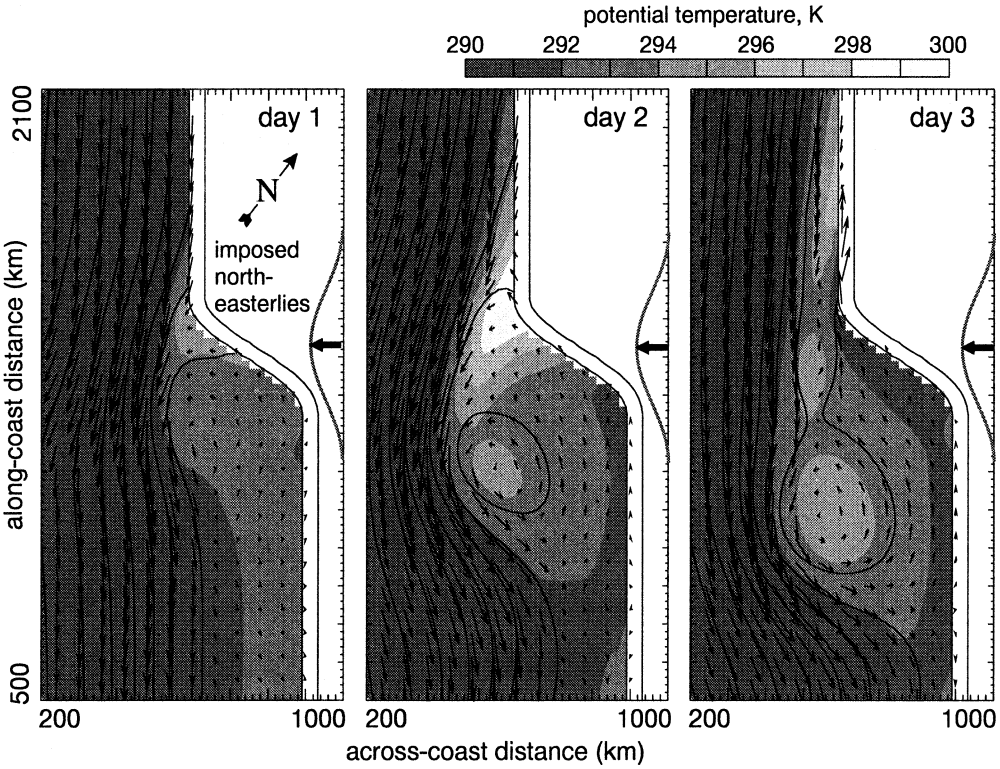

FIG. 4. Horizontal cross sections at $z = 250$ m for the simulation using an imposed northeasterly flow (the CTD simulation). Contoured as in Fig. 2.

in our idealized simulations. In order to examine the possible effects of taller mountains in this idealization of the Catalina eddy, we have performed simulations where we add an isolated ridge to the plateau used in the previous simulations. The ridge is located on the northeastern edge of the bight, and its maximum height above sea level is 1200 m. Figure 6 shows the ridge and the results from a simulation using this terrain for an imposed northwesterly flow; the simulation setup is identical to that depicted in Fig. 2, except for the addition of the ridge.

The flow evolution is similar to that for the Catalina eddy simulation shown in Fig. 2; the depression forms in the bight followed by a closed eddy. As is the case in the previous simulation (Fig. 2), the CTD that accompanies the eddy does not propagate out of the bight because it encounters the climatological northwesterly marine-layer flow at the northwest corner of the bight. The central marine-layer depression, coastal marine-layer elevation, and eddy circulation are slightly stronger in this case due to the enhanced lee troughing associated with the higher terrain of the ridge.

Simulations with an imposed northeasterly flow largely reproduce the CTD simulation depicted in Fig. 4 and, as in the case for the Catalina eddy simulations, show a slight enhancement of the eddy and CTD flow due to the enhanced lee troughing associated with the higher terrain.

5. Potential vorticity perspective

The Catalina eddy is a mesoscale feature, and in its mature state represents a quasi-balanced feature in these simulations. Thus, it is natural to consider the evolution of this feature from a potential vorticity (PV) perspective. The question that immediately arises concerning the eddy circulation is whether it is the result of a redistribution of PV existing in the base state, or rather the result of PV produced during the course of the simulation. Significant PV exists in the base state associated with the marine layer inversion, the northwesterly flow and the earth's rotation (see the bottom panel of Fig. 1). The simulations presented here are largely inviscid and the lower boundary is free slip. However, there is necessarily dissipation associated with the the leading edge of the propagating CTD found in the solutions. With regards to PV, the dissipation processes will produce PV.

Figure 7 shows horizontal cross sections of velocity vectors and PV at $z = 250$ m for days 1 through 3. At day 1 the marine-layer depression formed by the imposed northwesterly flow in the bight is associated with positive PV. This increase in PV occurs because the marine-layer inversion is being depressed, and we see the higher PV values associated with the inversion base. The initial PV structure is depicted in the lowest panel in Fig. 1, and the 250-m level is located just below the

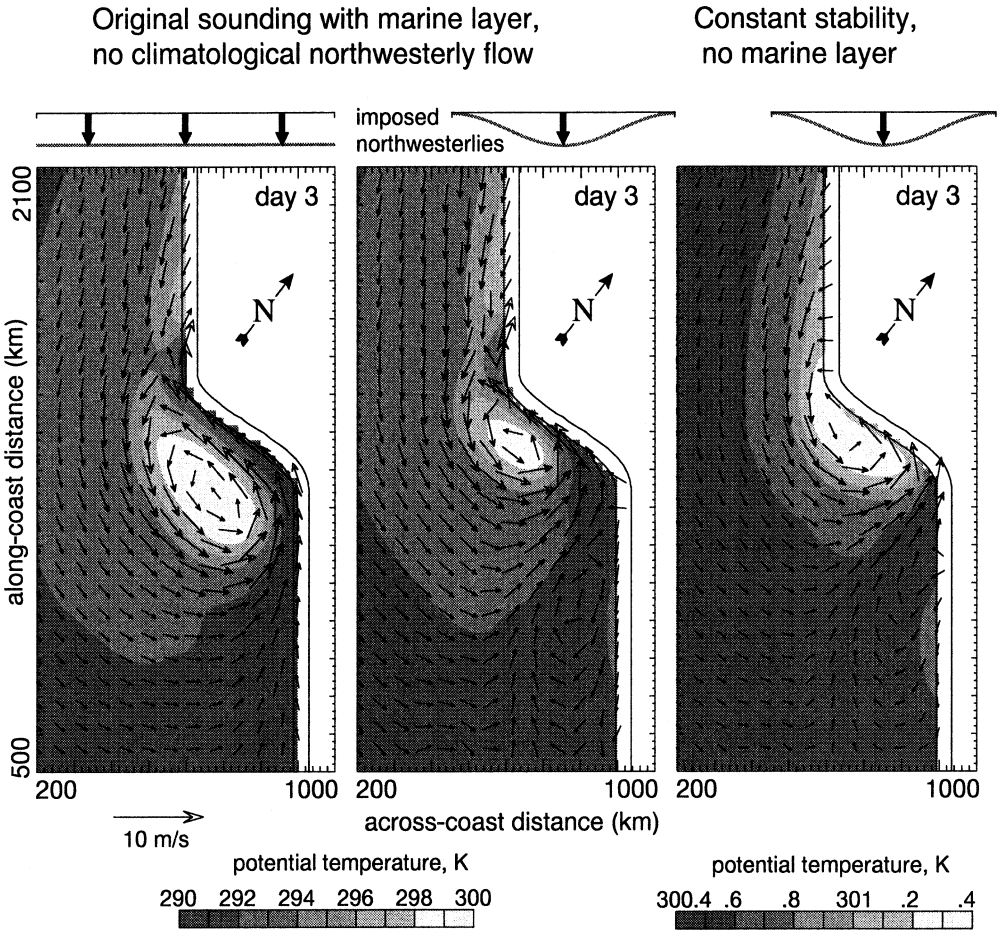

FIG. 5. Horizontal cross sections at $z = 250$ m at day 3 for simulations using an imposed northwesterly flow and a flat marine inversion (left and middle), and constant stability (no marine inversion; right). The left and middle plots depict simulations that vary only in the horizontal extent of the imposed flow. Contoured as in Fig. 2.

inversion and below the positive PV anomaly at the initial time. The marine layer is farther depressed by day 2, and now we see a ring of PV. The higher values of PV are those from air above the marine inversion. The only significant PV generation in this simulation is associated with dissipation at the leading edge of the CTD, found halfway up the coast in the bight at day 2. As this PV anomaly (marking the leading edge of the CTD) encounters the climatological northerlies between days 2 and 3, it is swept towards the south and entrained in the cyclonic eddy circulation. This PV anomaly is small and isolated and is not responsible for the mesoscale eddy circulation.

Thus, a potential vorticity description of the Catalina eddy formation in this simulation would emphasize the redistribution of PV existing in the initial state in the marine layer; the generation of PV is localized to the leading edge of the CTD and does not play a significant role in these simulations of Catalina eddies. Moreover, simulations that begin with uniform stratification, no marine layer, and no marine-layer flow, will still produce an eddy in the bight, similar to the low pressure produced in the CTD simulations using constant stratification in Skamarock et al. (1999, see their Fig. 14). PV anomalies are not needed to produce an eddy in CTD and Catalina eddy simulations—they appear in simulations using constant PV environments.

6. Summary and discussion

Using simulations in an idealized environment representing the southern California bight and it surroundings, we have illustrated several points concerning Catalina eddies and the CTDs that often accompany these eddies.

- The Catalina eddy can be formed by lee troughing, as found in previous observational and modeling studies (e.g. Bosart 1983; Mass and Albright 1989; and others), and CTDs along the west coast and Catalina eddies both share lee troughing as an essential dynamical precursor.

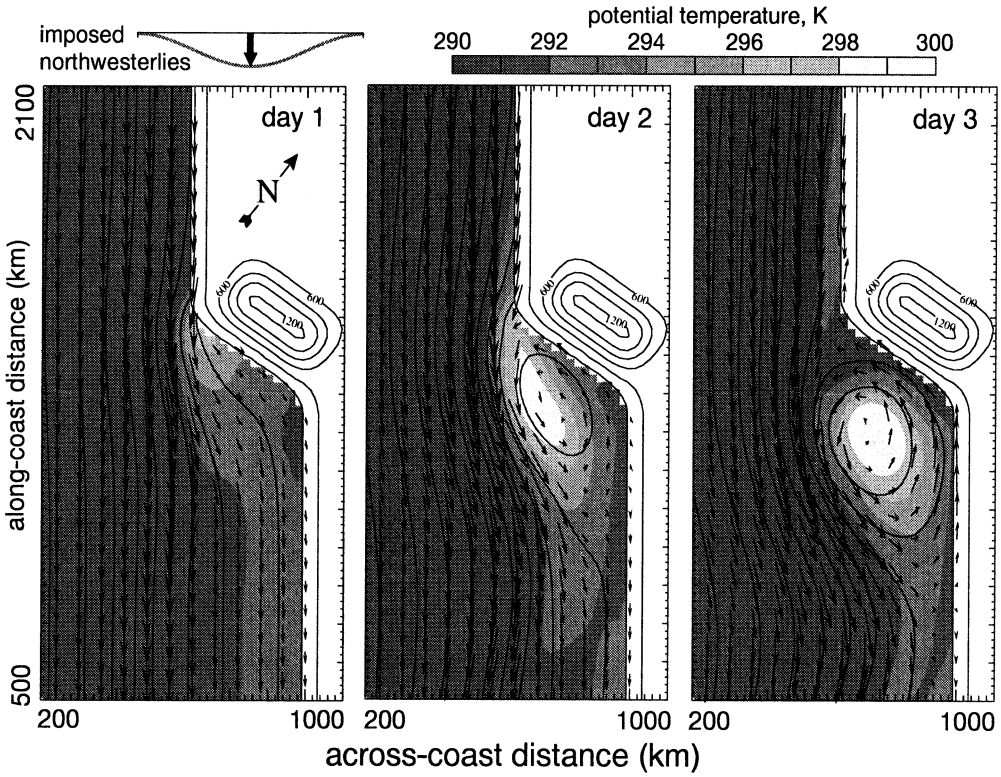

FIG. 6. Horizontal cross sections at $z = 250$ m for the simulation using an imposed northwesterly flow (the Catalina eddy simulation) with the addition of a ridge north of the bight. Contoured as in Fig. 2.

- Eddies and CTDs are produced provided that 1) there is sufficient stratification in the environment; 2) the offshore flow is of sufficient strength, breadth, and duration; and 3) there is sufficient terrain to produce significant lee troughing. Details of the marine-layer structure, terrain, and offshore flow are secondary effects for eddy and CTD formation.
- Whether or not the CTDs that are formed in conjunction with Catalina eddies can escape the bight region and propagate farther up the California coast is largely dependent on the direction and strength of the synoptic-scale offshore flow.
- From a PV perspective, PV generation during the course of eddy formation plays no significant role in producing the eddy. Also, horizontal vorticity in the initial marine-layer flow and in the imposed offshore flow play no significant role in producing the eddy.

Other studies have shown that effects arising from the diurnal cycle, the planetary boundary layer over land, details of the topography surrounding the bight, and mesoscale details associated with a particular event can modulate the Catalina eddy and CTD. Using simulations possessing realistic topography but with initially uniform geostrophic winds, Ulrickson et al. (1995) find that an eddy forms in the southern California bight due to lee troughing, and that no eddy forms when the terrain is removed from the simulation. They also find that diurnal effects (not considered in the present study) can change the timing and intensity of the eddy, but do not effect whether or not an eddy will form. Davis et al. (2000), using real data MM5 simulations of the 26–30 June 1988 Catalina eddy, find that the Catalina eddy can be strongly modulated by the diurnal cycle through boundary layer effects upwind (north) of the bight; the diurnally modulated boundary layer on the land upwind of the bight results in high Froude number flow over the mountain later in the day that descends in the lee; whereas, the nighttime boundary layer cooling leads to flow predominantly around the mountain, and no significant troughing in the lee. They also find that the appearance of a mature eddy is linked to a weakening of the large-scale northwesterlies such that vorticity generated by lee troughing in the bight is not swept southward out of the bight.

The simulations presented in this study represent the simplest idealization of Catalina eddy and CTD dynamics while still using fully compressible equations. As such, the simulations illuminate the essential dynamics of the Catalina eddy and provide a clear dynamical linkage between CTDs and Catalina eddies. Other effects arising from the diurnal cycle, the planetary boundary layer over land, details of the topography surrounding the bight, and mesoscale details associated with a particular event can significantly modulate the Catalina

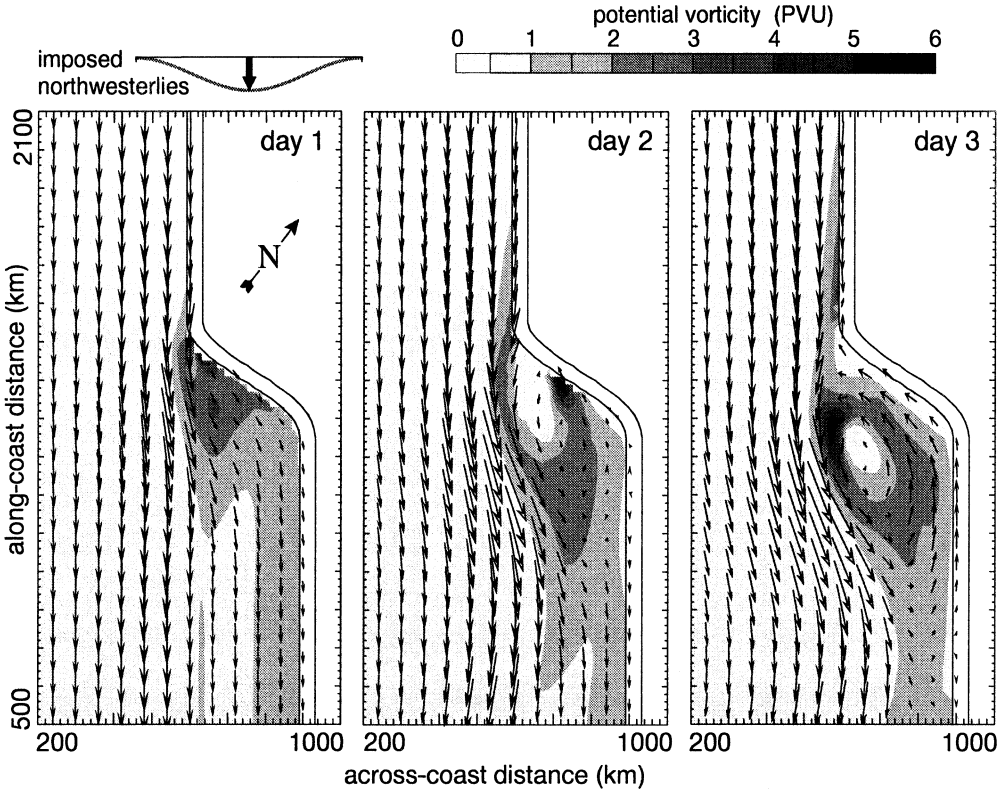

FIG. 7. Horizontal cross sections of PV and horizontal velocity vectors at $z = 250$ m for the simulation using an imposed northwesterly flow (the Catalina eddy simulation, also depicted in Fig. 2).

eddy and CTD. We believe that while these effects are important (especially for forecasting these events), they are secondary with respect to the essential dynamics of the Catalina eddy and the CTD.

Acknowledgments. This research is supported in part by the Office of Naval Research Grant N00014-97-1-0013.

REFERENCES

Bond, N. A., C. F. Mass, and J. E. Overland, 1996: Coastally trapped wind reversals along the United States west coast during the warm season. Part I: Climatology and temporal evolution. *Mon. Wea. Rev.*, **124,** 430–445.

Bosart, L. F., 1983: Analysis of a California Catalina eddy. *Mon. Wea. Rev.*, **111,** 1619–1633.

Davis, C., S. Low-Nam, and C. F. Mass, 2000: Dynamics of a Catalina eddy revealed by numerical simulation. *Mon. Wea. Rev.*, **128,** 2885–2904.

Dorman, C. E., 1985: Evidence of Kelvin waves in California's marine layer and related eddy generation. *Mon. Wea. Rev.*, **113,** 827–839.

——, and C. D. Winant, 2000: The marine layer in and around the Santa Barbara Channel. *Mon. Wea. Rev.*, **128,** 261–282.

——, T. Holt, D. P. Rogers, and K. Edwards, 2000: Large-scale structure of the June–July 1996 marine boundary layer along California and Oregon. *Mon. Wea. Rev.*, **128,** 1632–1652.

Durran, D. R., and J. B. Klemp, 1983: A compressible model for the simulation of moist mountain waves. *Mon. Wea. Rev.*, **111,** 2341–2361.

Mass, C. F., and M. D. Albright, 1989: Origin of the Catalina eddy. *Mon. Wea. Rev.*, **117,** 2406–2436.

——, and N. A. Bond, 1996: Coastally trapped wind reversals along the United States west coast during the warm season. Part II: Synoptic evolution. *Mon. Wea. Rev.*, **124,** 446–461.

Neiburger, M., D. S. Johnson, and C.-W. Chien, 1961: *Studies of the Structure of the Atmosphere over the Eastern Pacific Ocean in the Summer*. University of California Press, 94 pp.

Pierrehumbert, R. T., 1986: Lee cyclogenesis. *Mesoscale Meteorology and Forecasting*, P. S. Ray, Ed., Amer., Meteor., Soc., 509–511.

Ralph, F. M., L. Armi, J. M. Bane, C. Dorman, W. D. Neff, P. J. Neiman, W. Nuss, and P. O. G. Persson, 1998: Observations and analysis of the 10–11 June 1994 coastally trapped disturbance. *Mon. Wea. Rev.*, **126,** 2435–2465.

Skamarock, W. C., R. Rotunno, and J. B. Klemp, 1999: Models of coastally trapped disturbances. *J. Atmos. Sci.*, **56,** 3349–3365.

Thompson, W. T., S. D. Burk, and J. Rosenthal, 1997: An investigation of the Catalina eddy. *Mon. Wea. Rev.*, **125,** 1135–1146.

Ueyoshi, K., and J. O. Roads, 1993: Simulation and prediction of the Catalina eddy. *Mon. Wea. Rev.*, **121,** 2975–3000.

Ulrickson, B. L., J. S. Hoffmaster, J. Robinson, and D. Vimont, 1995: A numerical modeling study of the Catalina eddy. *Mon. Wea. Rev.*, **123,** 1364–1373.

Wakimoto, R., 1987: The Catalina eddy and its effect on pollution in Southern California. *Mon. Wea. Rev.*, **115,** 837–855.

Williamson, L. D., and P. J. Rasch, 1989: Two-dimensional semi-Lagrangian transport with shape-preserving interpolation. *Mon. Wea. Rev.*, **117,** 102–129.

Zemba, J., and C. A. Friehe, 1987: The marine atmospheric boundary layer jet in the coastal ocean dynamics experiment. *J. Geophys. Res.*, **92,** 1489–1496.